Mon. Not. R. Astron. Soc. **000**, 1–9 (2012) Printed 17 May 2013 (MN LATEX style file v2.2)

Empirical Constraints on the Star Formation & Redshift Dependence of the Lyα 'Effective' Escape Fraction

Mark Dijkstra[1⋆] and Akila Jeeson-Daniel[1,2]
[1] *Max Planck Institute for Astrophysics, Karl-Schwarzschild-Str. 1, 85741, Garching, Germany*
[2] *School of Physics, University of Melbourne, Parkville, Victoria, 3010, Australia*

17 May 2013

ABSTRACT

We derive empirical constraints on the volume averaged 'effective' escape fraction of Lyα photons from star forming galaxies as a function of redshift, by comparing star formation functions inferred directly from observations, to observed Lyα luminosity functions. Our analysis shows that the effective escape fraction increases from $f_{\rm esc}^{\rm eff} \sim 1-3\%$ at $z=0$, to $f_{\rm esc}^{\rm eff} \sim 10\%$ at $z=3-4$, and to $f_{\rm esc}^{\rm eff} = 35-50\%$ at $z=6$. Our constraint at $z=6$ lies above predictions by models that do not include winds, and therefore hints at the importance of winds in the Lyα transfer process (even) at this redshift. We can reproduce Lyα luminosity functions with an $f_{\rm esc}^{\rm eff}$ that does not depend on the galaxies star formation rates (ψ) over up to ~ 2 orders of magnitude in Lyα luminosity. It is possible to reproduce the luminosity functions with an $f_{\rm esc}^{\rm eff}$ that decreases with ψ - which appears favored by observations of drop-out galaxies - in models which include a large scatter ($\sigma \gtrsim 1.0$ dex) in $f_{\rm esc}^{\rm eff}$, and/or in which star forming galaxies only have a non-zero $f_{\rm esc}^{\rm eff}$ for a fraction of their life-time or a fraction of sightlines. We provide a fitting formula that summarizes our findings.

Key words: line: formation–radiative transfer–galaxies: intergalactic medium–galaxies: ISM–ultraviolet: galaxies – cosmology: observations

1 INTRODUCTION

The Lyα emission line is one of the most prominent features in the intrinsic spectrum of star forming galaxies (e.g. Partridge & Peebles 1967; Schaerer 2003; Johnson et al. 2009). The presence of a luminous, redshifted Lyα line has been used to spectroscopically confirm - and find - galaxies out to $z \sim 7$ (e.g. Iye et al. 2006; Ota et al. 2010; Rhoads et al. 2012).

Lyα emitting galaxies (LAEs hereafter)[1] are of interest for various reasons, including for example: (*i*) their continua are typically fainter than - and hence complement samples of- continuum selected (i.e. drop-out selected) galaxies; (*ii*) LAEs at $z>5$ provide an independent probe of the reionization epoch, as the Lyα line is affected by neutral intergalactic gas (e.g. Haiman & Spaans 1999; Malhotra & Rhoads 2004); (*iii*) as Lyα photons likely scatter through the interstellar media (ISM) of galaxies, the total distance they travel through the ISM is enhanced compared to that of continuum photons. Lyα photons are therefore thought to provide a sensitive probe of the dust content (and gas kinematics) of the ISM; (*iv*) Lyα selected galaxies will be used to probe the equation of state of the dark energy at $z=1.9-3.5$ by the HETDEX[2] experiment (Hill et al. 2008).

The main uncertainty that affects interpretations of Lyα observations of LAEs relates to the complex radiative transfer of Lyα photons through both the ISM, the circum galactic medium (CGM), and intergalactic medium (IGM, e.g. Zheng et al. 2010; Dijkstra & Kramer 2012; Verhamme et al. 2012; Laursen et al. 2012; Cantalupo et al. 2012; Jeeson-Daniel et al. 2012). Moreover, these processes are not independent: radiative transfer at the ISM-level affects how the radiative transfer proceeds at the intergalactic level[3]. In recent years Lyα RT has been modeled on all these scales, usually by combining simulated galax-

⋆ E-mail:dijkstra@mpa-garching.mpg.de

[1] In this letter, we use the term LAE to describe any Lyα emitting galaxy. It is also common in the literature to define LAEs as only those Lyα emitting galaxies that have been selected on the basis of their strong Lyα emission line.

[2] http://www.hetdex.org

[3] The simplest way to illustrate this dependence is by considering that scattering of Lyα photons through outflows of HI gas (on - say - kpc scales) results in an overall redshift of the Lyα spectral line relative to other nebular lines (e.g. Zheng & Miralda-Escudé 2002; Dijkstra et al. 2006; Verhamme et al. 2008). This overall redshift of the Lyα line reduces the probability that these photons subsequently scatter in the IGM (Dijkstra & Wyithe 2010).

ies with Lyα radiative transfer calculations (e.g Tasitsiomi 2006; Laursen & Sommer-Larsen 2007; Barnes et al. 2011; Verhamme et al. 2012; Yajima et al. 2012). These calculations are extremely difficult to carry out from first principles (see Dijkstra & Kramer 2012), and ultimately must be constrained by observations.

The goal of this paper is to provide empirical (i.e. based purely on observations) constraints on the dependence of the *effective escape fraction*[4] of Lyα photons, $f_{\rm esc}^{\rm eff} \equiv L_\alpha/L_{\alpha,\rm int}$, where L_α ($L_{\alpha,\rm em}$) denotes the observed (intrinsic) Lyα luminosity. Our goal is to constrain $f_{\rm esc}^{\rm eff}$ as a function of redshift (as in Hayes et al. 2011; Blanc et al. 2011). Furthermore, we investigate whether $f_{\rm esc}^{\rm eff}$ depends on the star formation rate of galaxies. Previous works by Hayes et al. (2011) and Blanc et al. (2011) constrained the volume averaged effective escape fraction $f_{\rm esc}^{\rm eff}$ by comparing the star formation rate density, $\dot\rho_*$, inferred from the *observed* Lyα luminosity density, to $\dot\rho_*$ inferred from other observations. This method is highly non-trivial, because Lyα observations only detect galaxies for which $f_{\rm esc}^{\rm eff}$ exceeds some star formation rate-dependent value (at very low star formation rates, the Lyα flux falls below the detection threshold even when all Lyα photons made it to the observer), and one must attempt to account for this. For example, Hayes et al. (2011) use UV-luminosity functions of drop-out galaxies to estimate the appropriate value for $\dot\rho_*$ at $z \gtrsim 2.5$, and a significant part of their analysis is devoted to choosing the proper lower integration limit when integrating over the UV-luminosity function. Our method uses star formation rate functions to estimate $f_{\rm esc}^{\rm eff}$. We show that this allows for more direct constraints which circumvent the difficulties associated with choosing such integration limits.

The outline of this paper is as follows: We describe in § 2 how we combine observations of Lyα luminosity functions of LAEs with observations of star formation functions, to put constraints on the effective escape fraction of Lyα photons, $f_{\rm esc}^{\rm eff}$. We present our main results in § 3 before presenting our conclusions in § 5.

2 EMPIRICAL CONSTRAINTS ON THE LYα EFFECTIVE ESCAPE FRACTION

Lyα photons - just as Hα photons - are emitted following recombination events in HII regions, and closely trace ongoing star formation. The Hα luminosity of a galaxy is related to its star formation rate, denoted with ψ, as $L_{\rm H\alpha} = 1.2\times10^{41}\times(\psi/[{\rm M_\odot\ yr^{-1}}])$ erg s^{-1} (Kennicutt 1998, this conversion assumes a Salpeter IMF in the mass range 0.1-100 $M_\odot$). The intrinsic Lyα luminosity, denoted with $L_{\alpha,\rm int}$, is $\sim 8\times$ larger than the Hα luminosity (for case-B recombination and $T = 10^4$ K, e.g. Hayes et al. 2011), and we have

$$L_{\alpha,\rm int} = k \times \Big(\frac{\psi}{M_\odot\ {\rm yr}^{-1}}\Big), \qquad (1)$$

where $k = 10^{42}$ erg s^{-1}. The factor k can be higher (or lower) by a factor of ~ 2 depending on the assumed IMF, and/or stellar metallicity. In the extreme case of a top-heavy IMF and zero-metallicity stars, the factor k can be as high as $k \approx 10$ (Raiter et al. 2010). Our main results scale with our assumed k as $f_{\rm esc}^{\rm eff} \propto k^{-1}$. The 'observed Ly$\alpha$ luminosity', defined as the observed flux multiplied by $4\pi d_{\rm L}^2(z)$ ($d_{\rm L}(z)$ denotes the luminosity distance out to redshift z), is

$$L_\alpha = f_{\rm esc}^{\rm eff}(\psi, z)\times L_{\alpha,\rm int}, \qquad (2)$$

where $f_{\rm esc}^{\rm eff}(\psi,z)$ denotes the effective escape fraction of Lyα photons.

We constrain the parameter $f_{\rm esc}^{\rm eff}(\psi,z)$ by comparing observed Lyα luminosity functions to observationally inferred star formation functions: the Lyα luminosity function, denoted by $\frac{dn}{d\log L_\alpha} d\log L_\alpha$, measures the comoving number density of galaxies with (the logarithm of their) Lyα luminosities in the range $\log L_\alpha \pm d\log L_\alpha/2$. The star formation function, denotes with $\frac{dn}{d\log\psi} d\log\psi$ denotes the comoving number density of galaxies that are forming stars at rate (whose logarithm is) in the range $\log\psi \pm d\log\psi/2$. We describe the star formation functions used in our analysis, and how we convert these into Lyα luminosity functions in § 2.1. This conversion depends on $f_{\rm esc}^{\rm eff}(\psi,z)$, and we use observed Ly$\alpha$ luminosity functions to obtain constraints in § 3.

2.1 Star Formation Functions

Star formation functions can be described by Schechter functions:

$$\frac{dn}{d\log\psi} = \ln 10 \times \psi \times \frac{\Phi_*}{\psi_*}\Big(\frac{\psi}{\psi_*}\Big)^{-\alpha}\exp(-\psi/\psi_*). \qquad (3)$$

We adopt the redshift dependent Schechter function parameters from Smit et al. (2012, their Table 3)[5]. Our results are insensitive to this choice (see § 4.3).

In the absence of scatter, there is a one-to-one relation between ψ and L_α. The Lyα luminosity functions then relate to the star formation functions as

$$\frac{dn}{d\log L_\alpha} = \frac{dn}{d\log\psi}\frac{d\log\psi}{d\log L_\alpha} = \frac{dn}{d\log\psi}\Big|_{\psi = L_\alpha/(k f_{\rm esc}^{\rm eff})}, \qquad (4)$$

where in the last equality we used Eq 1 and Eq 2.

In reality we do not expect each galaxy that forms stars at some rate ψ to have exactly the same $f_{\rm esc}^{\rm eff}$. It is therefore reasonable to study models in which we assume that there is a dispersion (or scatter) in $f_{\rm esc}^{\rm eff}$ at a fixed ψ. In the presence of scatter, we generally have

$$\frac{dn}{d\log L_\alpha} = \int_{-\infty}^{\infty} d\log\psi\ \frac{dn}{d\log\psi} P(\log L_\alpha|\log\psi) \qquad (5)$$

where $P(\log L_\alpha|\log\psi)d\log L_\alpha$ denotes the probability that a galaxy that is forming stars at a rate ψ has a Lyα luminosity in the range $\log L_\alpha \pm d\log L_\alpha/2$. We assume that the

[4] The term 'effective escape fraction' was coined previously by Nagamine et al. (2010), and is often simply referred to as 'escape fraction'. In § 4.1 we argue why we caution against universal usage of the term escape fraction, and why it helps to distinguish between an escape fraction and an effective escape fraction.

[5] For the data at $z = 0.35$ we use the values from Bell et al. (2007). For the data at $z = 0.35$ Bell et al. (2007) combine UV and MIR luminosity functions to construct their star formation functions. For the higher redshift star formation functions, Smit et al. (2012) construct star formation functions from UV LFs, combined with constraints on the slope of the rest-frame continuum β.

effective escape fraction $f_{\rm esc}^{\rm eff}$ has a scatter that is described by a (truncated) log-normal distribution. That is,

$$P(\log L_\alpha|\log\psi) \equiv \frac{dP}{d\log L_\alpha} = \frac{dP}{d\log f_{\rm esc}^{\rm eff}}\Big|_{f_{\rm esc}^{\rm eff}=L_\alpha/(k\psi)} = \\ = \begin{cases} \frac{\mathcal{N}}{\sqrt{2\pi}\sigma}\exp\left(\frac{-(\log f_{\rm esc}^{\rm eff}-\langle\log f_{\rm esc}^{\rm eff}\rangle)^2}{2\sigma^2}\right) & f_{\rm esc}^{\rm eff}\leqslant 1 \\ 0 & f_{\rm esc}^{\rm eff}>1 \end{cases},$$

where $\mathcal{N}$ denotes a factor that ensures that the function $dP/d\log f_{\rm esc}^{\rm eff}$ is normalized.

2.2 Constraining the Effective Escape Fraction.

We first assume that $f_{\rm esc}^{\rm eff}(z,\psi) = f_{\rm esc}^{\rm eff}(z)$. That is, we first assume that $f_{\rm esc}^{\rm eff}$ is independent of the star formation rate ψ. We make this assumption because we will show later that the Lyα luminosity functions are - surprisingly - consistent with this assumption.

Our analysis focusses on the Lyα luminosity functions centered on $z = 0.35$ from Deharveng et al. (2008, *red filled circles*) and Cowie et al. (2010, *blue filled squares*), $z = 3.1$, $z = 3.7$, and $z = 5.7$ from Ouchi et al. (2008, *red filled circles*) and Cassata et al. (2011, *blue filled squares).* At each redshift, we compute the posterior probability for a range of $f_{\rm esc}^{\rm eff}$ as $P(f_{\rm esc}^{\rm eff}) \propto \int d^3\mathbf{X}\,\mathcal{L}[f_{\rm esc}^{\rm eff}]P(f_{\rm esc}^{\rm eff})P_{\rm s}(\mathbf{X})$, where $\mathcal{L}[f_{\rm esc}^{\rm eff}] = \exp[-0.5\chi^2]$ denotes the likelihood, in which $\chi^2 = \sum_i^{N_{\rm data}}(\mathrm{model}_i - \mathrm{data}_i)^2/\sigma_i^2$. The function $P(f_{\rm esc}^{\rm eff}) \equiv 1$ denotes the prior probability distribution for $f_{\rm esc}^{\rm eff}$: i.e. we assume no prior knowledge of $f_{\rm esc}^{\rm eff}$. We stress however that our results do not depend on our choice of prior.

Finally, the vector $\mathbf{X}$ contains the three Schechter function parameters $\mathbf{X}^T = (\alpha, \psi_*, \Phi_*)$. The function $P_{\rm s}(\mathbf{X})$ describes the prior probability for having any combination of parameters: we assumed that $P_{\rm s}(\mathbf{X})$ is a multivariate Gaussian, i.e. $P_{\rm s}(\mathbf{X}) = \mathcal{N}\exp\Big[-\frac{1}{2}(\mathbf{X}-\mu_X)^T\mathbf{C}^{-1}(\mathbf{X}-\mu_X)\Big]$, where $\mathcal{N}$ denotes the normalization factor. The vector μ_X contains the best fit values for each of the parameters. The covariance matrix $\mathbf{C}$ contains the measured uncertainties on the parameters[6] (the most likely values and their uncertainties were taken from Smit et al. 2012).

3 RESULTS

3.1 No Scatter

Figure 1 shows four panels, each of which corresponds to one redshift bin. The observed Lyα luminosity functions that we used in our analysis are shown as the datapoints. The *inset* in each panel shows $\mathcal{L}[f_{\rm esc}^{\rm eff}]$ as a function of $f_{\rm esc}^{\rm eff}$. These panels contain two lines, both of which were obtained by fitting to a single data set. For example, we obtained the *black solid line* (*red dashed line*) in the $z = 0.35$ panel by fitting to the data from Deharveng et al. (2008) (Cowie et al. 2010)[7]. At each redshift, we show the model luminosity functions for which both $\mathcal{L}[f_{\rm esc}^{\rm eff}]$-curves are maximized, using the same line color and style.

The *upper left panel* shows that the data from Deharveng et al. (2008) translates to $f_{\rm esc}^{\rm eff} = 8.5 \pm 3\%$, while the data from Cowie et al. (2010) implies $f_{\rm esc}^{\rm eff} = 3^{+2}_{-1}\%$ at $z = 0.35$. Here the errorbars denote 68% confidence levels, where we use the so-called 'shortest interval' method (see Andrae 2010, and references therein) to determine the confidence intervals. The *upper right panel* shows that the effective escape fraction increases to $f_{\rm esc}^{\rm eff} = 17 \pm 5\%$ [$f_{\rm esc}^{\rm eff} = 10 \pm 3\%$] for the Ouchi et al. (2008) [Cassata et al. (2010)] data at $z = 3.1$, and to $f_{\rm esc}^{\rm eff} = 17^{+6}_{-4}\%$ [$f_{\rm esc}^{\rm eff} = 8 \pm 3\%$] for the Ouchi et al. (2008) [Cassata et al. 2010] data at $z = 3.7$. Finally, we find that the effective escape fraction increases to $f_{\rm esc}^{\rm eff} = 57^{+34}_{-21}\%$ [$f_{\rm esc}^{\rm eff} = 44^{+28}_{-22}\%$] for the Ouchi et al. (2008) data [Cassata et al. (2010)] at $z = 5.7$.

Our quoted uncertainties are statistical only, and do not take into account systematic uncertainties associated with the determination of observed Lyα luminosity functions. The different constraints we obtain on $f_{\rm esc}^{\rm eff}$ from different data-sets may reflect these systematic uncertainties: in particular, at $z \geqslant 3.1$ the data from Ouchi et al. (2008) derive from a narrow-band survey for LAEs, while the data from Cassata et al. (2010) derive from a deep spectroscopic survey (see § 4.3 for a more detailed discussion of systematic uncertainties).

Figure 1 shows that our models reproduce the individual datasets of observed Lyα luminosity functions well. Different datasets can result in slightly different constraints on $f_{\rm esc}^{\rm eff}$. It is striking that at $z \geqslant 3.1$ (especially $z = 3.1$ and $z = 5.7$), a ψ-independent $f_{\rm esc}^{\rm eff}$ reproduces the observations well over up to two orders Lyα luminosity, and therefore ψ. If anything, our models do not produce enough bright LAEs, which could be solved by having $f_{\rm esc}^{\rm eff}$ *increase* with ψ. Note however, that Ouchi et al. (2008) point out that the bright end (i.e. at $\log L_\alpha \gtrsim 43.4$) may be contaminated by low luminosity AGN. The only data-set that we cannot reproduce well is that of Cowie et al. (2010): our model predicts significantly fewer LAEs than their two data-points at $\log L_\alpha \gtrsim 42.3$. This discrepancy could again be (partially) resolved by having $f_{\rm esc}^{\rm eff}$ increase with ψ. As we show below (in § 3.2), we also significantly improve the agreement with the data when we introduce a scatter in $f_{\rm esc}^{\rm eff}$.

3.2 With Scatter

Figure 2 shows the same as Figure 1, but here the models include a dispersion in $f_{\rm esc}^{\rm eff}$ (Eq 5), which is described by a (truncated) log-normal distribution with a standard deviation of $\sigma = 0.5$. This choice for σ is a bit arbitrary, but can be justified by the work of Dijkstra & Westra (2010), who

[6] The covariance matrix in this case is a 3×3 matrix whose entries are given by $C_{ij} = \sigma_i\sigma_j\rho_{ij}$. Here σ_i denotes the uncertainty on parameter 'i', and ρ_{ij} denotes the correlation coefficient between parameter i and j, and obey $\rho_{ij} = \rho_{ji}$. These correlation coefficients are generally not given. Following Dijkstra & Wyithe (2012) we assumed that $\rho_{\alpha,\psi_*} = \rho_{\psi_*,\Phi_*} = \rho_{\alpha,\Phi_*} = 0.9$ at each redshift. By definition $\rho_{ii} = 1$ for all 'i'.

[7] The origin of the difference between the luminosity functions derived by Deharveng et al. (2008) and Cowie et al. (2010) appears to be in the incompleteness correction, which is large in Deharveng et al. (2008), but not in Cowie et al. (2010). Cowie et al. (2010) note that this difference may be caused by a missing color correction in the Deharveng analysis (and quote private communication).

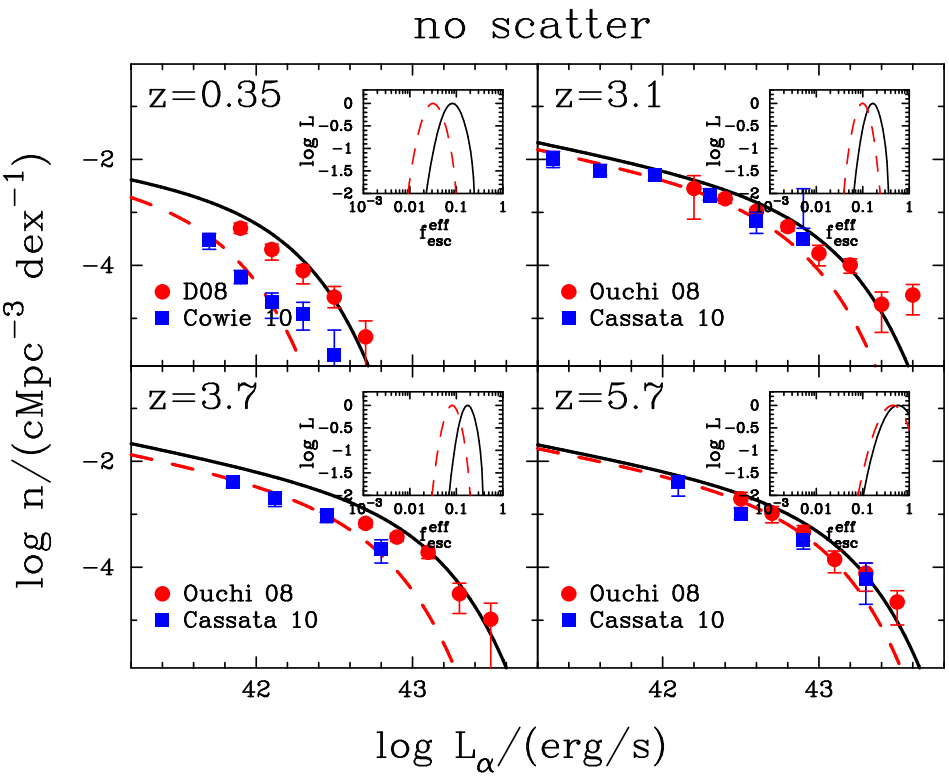

Figure 1. The Figure compares observed Lyα luminosity functions (indicated by the data points) of LAEs at $z = 0.35$ (*upper left*), $z = 3.1$ (*upper right*), $z = 3.7$ (*lower left*), and $z = 5.7$ (*lower right*) with model predictions under the assumption that there is a one-to-one relation between star formation rate ψ and observed Lyα luminosity L_α (see Eq 4, i.e. there is no scatter in $f_{\rm esc}^{\rm eff}$), for the best-fit observed Lyα fraction, $f_{\rm esc}^{\rm eff}$, (as *black solid lines* and *red dashed lines*, see text). The *insets* show the likelihood $\mathcal{L}[f_{\rm esc}^{\rm eff}]$ as a function of $f_{\rm esc}^{\rm eff}$. This Figure illustrates that the models reproduce the Lyα luminosity functions well, except at the bright end (which may be contaminated by low luminosity AGN, see Ouchi et al. 2008). It is worth pointing out that $f_{\rm esc}^{\rm eff}$ is independent of ψ in our models.

found that the ratio of the Lyα to the UV-derived star formation rate can be described by a log-normal distribution with $\sigma = 0.4$. We stress that changes to our main results are insignificant, even if we adopted $\sigma = 1.0$.

Figure 2 shows that a dispersion in $f_{\rm esc}^{\rm eff}$ flattens the predicted luminosity functions, and smoothens out the sharp-turnover in the predicted luminosity function. Both these changes help to improve the fit to the data at $z = 0.35$ (and also at the highest L_α data point at $z = 3.1$). Importantly, these models obtain constraints from different datasets that agree better with each other: for example, the best-fit models to the data from Ouchi et al. (2008) also provide decent fits to the data from Cassata et al. (2010).

In spite of the flattening of the predicted luminosity functions, these models still reproduce the data with an $\langle \log f_{\rm esc}^{\rm eff} \rangle$ that is independent of ψ. It is only when we adopt $\sigma \gtrsim 1.0$, that the predicted luminosity functions become flatter than the observations. For these models, the data would then require $\langle \log f_{\rm esc}^{\rm eff} \rangle$ to decrease with ψ. Such a requirement would be expected given observations of drop-out galaxies, which show evidence that the fraction of continuum selected galaxies that have 'strong' Lyα emission lines increases towards lower UV-luminosities (e.g. Stark et al. 2010). This suggests that Lyα photons have an easier time escape from galaxies with lower UV luminosities, and therefore likely from galaxies with lower star formation rates ψ.

The *insets* of Figure 2 show $\mathcal{L}(\langle \log f_{\rm esc}^{\rm eff} \rangle)$. For example, the *inset* in the *upper right panel* shows that the best-fit $\langle \log f_{\rm esc}^{\rm eff} \rangle$ at $z = 3.1$ is $10^{\langle \log f_{\rm esc}^{\rm eff} \rangle} \sim 0.06 - 0.1$, which lie a factor of ~ 1.7 below[8] the best-fit $f_{\rm esc}^{\rm eff}$ we derived for the model with no scatter. The best-fit values of $\langle \log f_{\rm esc}^{\rm eff} \rangle$ depend on the choice of σ: the larger σ, the smaller $\langle f_{\rm esc}^{\rm eff} \rangle$. The reason for this reduction is that at fixed $\langle \log f_{\rm esc}^{\rm eff} \rangle$, increasing σ increases the *expectation value* $E(f_{\rm esc}^{\rm eff})$, which is given by $E(f_{\rm esc}^{\rm eff}) = \int_0^1 df_{\rm esc}^{\rm eff}\ f_{\rm esc}^{\rm eff} \frac{dP}{df_{\rm esc}^{\rm eff}}$. We have verified that this best-fit expectation value $E(f_{\rm esc}^{\rm eff})$ barely depends on our choice of σ.

We now practically have three 'measures' of $f_{\rm esc}^{\rm eff}$ (namely $f_{\rm esc}^{\rm eff}$, $\langle \log f_{\rm esc}^{\rm eff} \rangle$, and $E(f_{\rm esc}^{\rm eff})$), which may be a bit confusing. We have therefore briefly summarized the meaning of these symbols in Table 1.

3.3 Comparing our $f_{\rm esc}^{\rm eff}(z)$ with Previous Works

We compare our inferred redshift evolution of $f_{\rm esc}^{\rm eff}(z)$ to the power-law fitting function from Hayes et al. (2011) in Figure 3. The *filled symbols* represent the constraints on $f_{\rm esc}^{\rm eff}$ that we obtained for the 'no-scatter' models in § 3.1. The

[8] At $z = 5.7$ the best-fit $\langle \log f_{\rm esc}^{\rm eff} \rangle$ lies above the best-fit $f_{\rm esc}^{\rm eff}$ that we inferred in the absence of scatter. This is because the expectation value, $E(f_{\rm esc}^{\rm eff})$, becomes *less* than $10^{\langle \log f_{\rm esc}^{\rm eff} \rangle}$ for $10^{\langle \log f_{\rm esc}^{\rm eff} \rangle} \gtrsim 0.3$ when $\sigma = 0.5$ for the truncated PDFs that we assign to $f_{\rm esc}^{\rm eff}$.

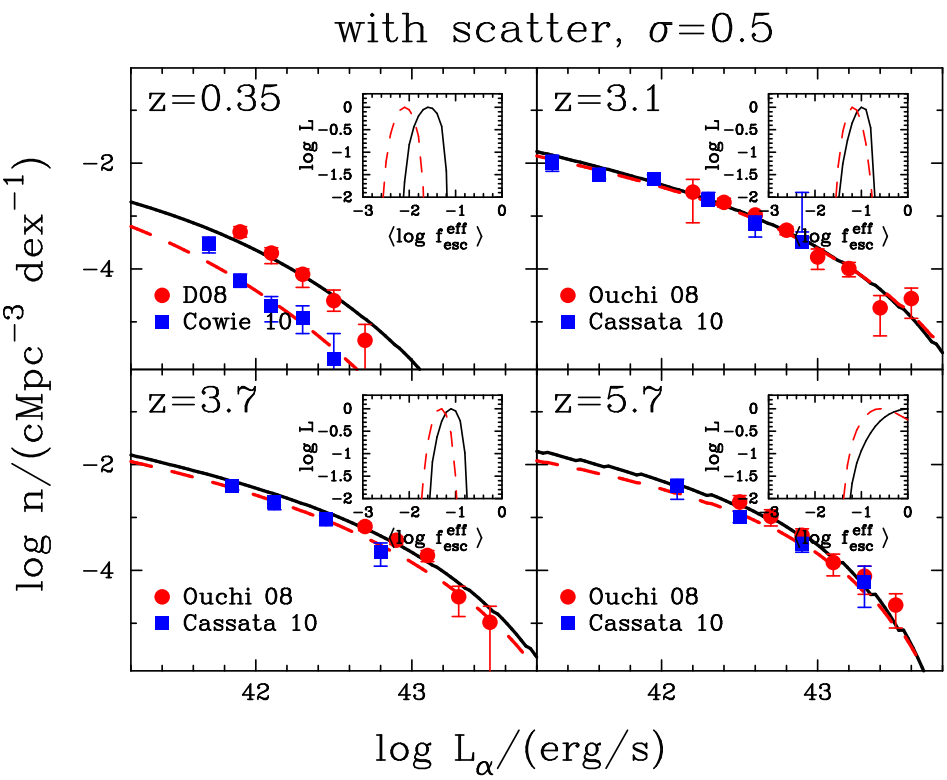

Figure 2. Same as Figure 1, but for models in which we assume that there is a dispersion in $f_{\rm esc}^{\rm eff}$, described by a log-normal distribution with a standard deviation of $\sigma = 0.5$, at a fixed ψ. This Figure shows that a dispersion in $f_{\rm esc}^{\rm eff}$ flattens the predicted Lyα luminosity functions, which improves the agreement with the data at $z = 0.35$ and at high L_α. These models obtain constraints from different datasets that agree better with each other.

Table 1. Summary of 'Different' Measures of $f_{\rm esc}^{\rm eff}$.

symbol	meaning
$f_{\rm esc}^{\rm eff}$	effective escape fraction of Lyα of a galaxy
$\langle \log f_{\rm esc}^{\rm eff} \rangle$	mean of log $f_{\rm esc}^{\rm eff}$ in a lognormal PDF (Eq 6)
$E(f_{\rm esc}^{\rm eff})$	expectation value of $f_{\rm esc}^{\rm eff}$ for models with a lognormal PDF

open symbols represent our constraints on the best-fit expectation value $E(f_{\rm esc}^{\rm eff})$ (these constraints do not depend on our adopted σ). At each redshift, we have two data points which correspond to different data sets. Including scatter reduces the expectation value of $f_{\rm esc}^{\rm eff}$ compared to models that have no scatter, typically by about $\sim 1-\sigma$. The reduction is a bit larger at $z = 0.35$. However, here we point out that the models that do not include scatter had difficulties fitting the data to begin with, and the constraints that we inferred from these models were likely less reliable.

Figure 3 shows that our best-fit values are consistent with Hayes et al. (2011) at $z \geqslant 3.1$, albeit on the high end of their quoted range. At $z = 0.35$, our constraints on $f_{\rm esc}^{\rm eff}$ lie significantly higher than those of Hayes et al. (2011), who found $f_{\rm esc}^{\rm eff} = 1.3 \pm 0.9\%$ using the data from Deharveng et al. (2008), and $f_{\rm esc}^{\rm eff} = 0.3 \pm 0.2\%$ using the data from Cowie et al. (2010). These values would clearly not allow us to reconstruct the observed Lyα luminosity functions.

A possible explanation for their lower preferred values for $f_{\rm esc}^{\rm eff}$ at $z = 0.35$ is that Hayes et al. (2011) compare the observed Lyα luminosity density to a total star formation rate density of $\dot{\rho}_* \sim 30 \times 10^{-3}$ M$_\odot$ yr^{-1} cMpc^{-3}. This value corresponds to the total integrated star formation rate density (see Table 1 of Bothwell et al. 2011). Bothwell et al. (2011) show that galaxies with $\psi \gtrsim 10$ M$_\odot$ yr^{-1} account only for $\sim 20\%$ of $\dot{\rho}_*$. If we consider an extreme example in which all galaxies with $\psi < 10$ M$_\odot$ yr^{-1} have $f_{\rm esc}^{\rm eff} = 3\%$, then their observed Ly$\alpha$ luminosity would be $L_\alpha \sim 3 \times 10^{41}$ erg s^{-1}, which lies below the minimum detectable Lyα luminosity. The luminosity function presented by Cowie et al. (2010) is therefore consistent with all galaxies $\psi < 10$ M$_\odot$ yr^{-1} having $f_{\rm esc}^{\rm eff} = 3\%$. Even if all galaxies with $\psi > 10$ M$_\odot$ yr^{-1} would have $f_{\rm esc}^{\rm eff} = 0$, then $f_{\rm esc}^{\rm eff}$ averaged over the population as a whole would be $\sim 2.4\%$, which is almost an order of magnitude higher than the value reported by Hayes et al. (2011). While the example we discussed here is clearly not realistic, it nevertheless shows that for very small $f_{\rm esc}^{\rm eff}$, large systematic uncertainties may be associated with estimating $f_{\rm esc}^{\rm eff}$ by comparing an observed Lyα luminosity density to a star formation rate density.

We have also indicated a (ad-hoc) fitting formula that we found to capture the redshift evolution of our inferred $f_{\rm esc}^{\rm eff}$ and its uncertainties reasonably well:

$$f_{\rm esc}^{\rm eff}(z, \psi) = a_1 + a_2 \exp(z^{0.7}). \quad (6)$$

, where $a_1 = 0.01^{+0.03}_{-0.01}$ and $a_2 = (12^{+8}_{-4}) \times 10^{-3}$. The median of this fitting formula is represented by the *black solid line* in Figure 2. The upper/lower boundary of the *grey region* represents our fitting formula when both a_1 and a_2 are

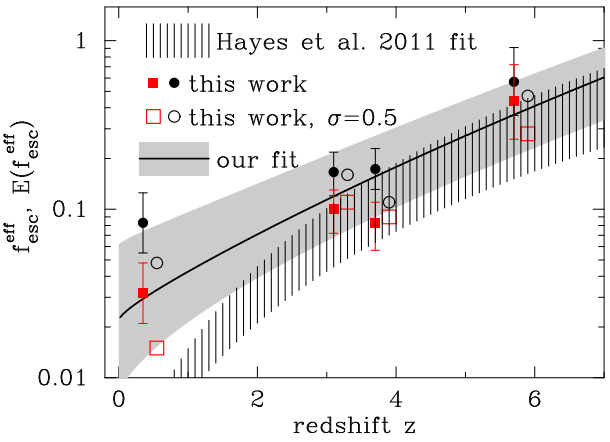

Figure 3. This Figure compares our constraints on $f_{\rm esc}^{\rm eff}$ with the analytic fitting formula provided by Hayes et al. (2011, indicated by the *black shaded region*). The *filled symbols* represent the constraints on $f_{\rm esc}^{\rm eff}$ for the 'no-scatter' models. The *open symbols* represent our constraints on the expectation values of $E(f_{\rm esc}^{\rm eff})$ for our models that include scatter. At each redshift, we have two data points which correspond to different data sets. The *grey region* represents our fitting formula (Eq 6) and its uncertainties. Our work is consistent with Hayes et al. (2011), except at $z = 0.35$ where our inferred $f_{\rm esc}^{\rm eff}$ is higher, which is likely related to systematic uncertainties (see text).

maximized/minimized. We stress that the uncertainties on the parameters a_1 and a_2 do not represent standard confidence levels. Instead, they simply mark the boundaries of our grey region. We obtained the power-law '0.7' in the exponential function after trial and error. The fitting formula Eq. 6 clearly captures our main results well, and further 'predicts' that $f_{\rm esc}^{\rm eff} \sim 7^{+7}_{-3}\%$ at $z = 2$, which is consistent with Hayes et al. (2010) who found $f_{\rm esc}^{\rm eff} = 5.3 \pm 3.8\%$ by comparing Lyα to Hα luminosity functions. We have also applied our analysis to the more recent $z \sim 1$ data of Barger et al. (2012, not shown here), and found $f_{\rm esc}^{\rm eff} = 5 \pm 1\%$, which is also captured by our fitting formula.

4 DISCUSSION

4.1 'Effective Escape' Fraction vs. 'Escape' Fraction

We explicitly differentiate between the term 'escape' fraction and 'effective escape' fraction, because these two quantities can take on very different values. In theoretical calculations that follow the transport of Lyα photons through a dusty medium, it is straightforward to compute the fraction of photons that are not absorbed by dust, and hence 'escape' (e.g. Neufeld 1990; Hansen & Oh 2006; Laursen & Sommer-Larsen 2007; Yajima et al. 2012; Laursen et al. 2012; Yajima et al. 2013). However, a large fraction of Lyα photons that escape from this medium can scatter in the surrounding circum-galactic and/or intergalactic medium and give rise to a low surface brightness Lyα glow around galaxies (e.g. Dijkstra et al. 2007; Zheng et al. 2010; Laursen et al. 2011; Zheng et al. 2011; Steidel et al. 2011; Jeeson-Daniel et al. 2012). The surface brightness of this scattered radiation is typically much fainter than can be observed[9], and this Lyα radiation would effectively be lost in observations. For example, Zheng et al. (2010) find that Lyα scattering in the ionized IGM at $z = 5.7$ rendered $80 - 95\%$ of all emitted Lyα radiation undetectable (consistent with the other studies, see § 4.4). There is no dust in their simulations, and the escape fraction of Lyα photons is 100%. In contrast, the effective escape fraction would only be $f_{\rm esc}^{\rm eff} \sim 5 - 20\%$.

There is also observational evidence for the existence of spatially extended low surface brightness Lyα emission around galaxies (e.g. Fynbo et al. 2001; Ostlin et al. 2009; Rauch et al. 2008; Steidel et al. 2011; Matsuda et al. 2012; Hayes et al. 2013). Steidel et al. (2011) detected spatially extended Lyα emission after stacking Lyα observations on 92 $z \sim 2.6$ LBGs, which allowed them to probe Lyα emission down to ~ 10 times fainter surface brightness levels. The total flux in their spatially extended halos significantly exceeded the total Lyα flux coming directly from their galaxies. The observations by Steidel et al. (2011) imply that the escape fraction of Lyα photons can exceed the effective escape fraction significantly for surface brightness thresholds that are typical for current observations. Similarly, Matsuda et al. (2012) detected Lyα halos around $z = 3.1$ LAEs and found that the size of the halos (at fixed UV-luminosity of the LAEs) increases with local density (measured by the number density of LAEs). This dependence may help explain why other groups have not detected[10] spatially extended Lyα halos around LAEs (e.g. Feldmeier et al. 2013). In any case, the *possibility* that there is more Lyα flux in diffuse Lyα halos than in a compact source illustrates that the effective escape fraction - and previous determinations of this quantity - depend on the surface brightness threshold of the survey of interest (or the size of the photometric aperture in fixed aperture photometry), while the escape fraction does not (also see Yajima et al. 2012).

The universal usage of the term escape fraction complicates comparisons between different studies: for example, Yajima et al. (2013) compute true Lyα escape fractions in simulated galaxies as a function of redshift. Similarly, semi-analytic studies that model LAEs at $z = 3 - 6$ (e.g. Kobayashi et al. 2007; Dayal et al. 2011; Shimizu et al. 2011; Forero-Romero et al. 2011) introduce an escape fraction, which corresponds to a true escape fraction. Caution must be exercised when comparing these escape fractions to the observationally inferred effective escape fractions (as in Hayes et al. 2011, Blanc et al. 2011, and in this paper). Moreover, in some (but not all) studies the constraints on $f_{\rm esc}$ (and/or $f_{\rm esc}^{\rm eff}$) involve a 'correction' for scattering in the IGM. We stress that this correction is highly uncertain, as

[9] For example, the surface brightness threshold for the $z = 5.7$ LAE survey by Ouchi et al. (2008) is $\sim 10^{-18}$ erg s^{-1} cm^{-2} arcsec^{-2}. Rauch et al. (2008) managed to go a factor of ~ 10 deeper in a ~ 100 hr exposure on the VLT.

[10] Recently, Jiang et al. (2013) did not detect spatially extended Lyα emission around stacks of 43 $z = 5.7$ LAEs, and 40 $z = 6.5$ LAEs. At these redshifts there is room to hide a significant Lyα flux in the halo, even for the surface brightness threshold of $\sim 10^{-19}$ erg s^{-1} cm^{-2} arcsec^{-2} that is reached in the stacking analysis. Jiang et al. (2013) comment that these observations indeed still appear broadly consistent with the predictions by Zheng et al. (2011).

it depends on the radiative transfer at the interstellar and circum-galactic level (see § 1).

4.2 Comparison to Previous Works

We already compared our results to those obtained by Hayes et al. (2011, and also Blanc et al. 2010). Our approach, in which we use star formation functions and Lyα luminosity functions to constrain $f_{\rm esc}^{\rm eff}$, is similar to that adopted in theoretical studies. For example, Le Delliou et al. (2006) use semi-analytic models - while e.g. Nagamine et al. (2010) use hydrodynamical simulations - to generate star formation functions[11], and then use Lyα luminosity functions to constrain $f_{\rm esc}^{\rm eff}$ at $z = 3-6$. Importantly, the models that are used to generate the theoretical star formation functions are typically constrained by observations. However, these (almost the same) observations can be converted directly into star formation functions, i.e. without generating the intermediate theoretical model. Indeed, our method completely circumvents this intermediate step. The fact that we can side-step this (substantial) part of the calculations allow us to more efficiently explore a larger suite of models for $f_{\rm esc}^{\rm eff}$, and to explore the impact of uncertainties with the observationally inferred star formation functions on our results.

Our results are broadly consistent with these previous theoretical studies: Nagamine et al. (2010) find that $f_{\rm esc}^{\rm eff} = 0.1$ at $z = 3.1$, which is in excellent agreement with our results. Nagamine et al. (2010) find $f_{\rm esc}^{\rm eff} = 0.15$ at $z = 6$, which is a factor of $\sim 2-3$ lower than what we find. The origin of this difference is unclear, but the *lower right panel* of Figure 2 shows that the value preferred by Nagamine et al. (2010) ($10^{\langle \log f_{\rm esc}^{\rm eff} \rangle} = 0.15$) is not ruled out at great significance. Le Delliou et al. (2006) find $f_{\rm esc}^{\rm eff} \sim 0.02$ at $z = 3-6$. However, a redshift-dependent fraction of stars form in bursts with a top-heavy IMF for which $k \sim 10$ (see § 2). Hayes et al. (2011) show that if this top-heavy IMF is replaced with a standard Salpeter IMF, then the constraints obtained by Le Delliou et al. (2006) agree well with Nagamine et al. (2010) at $z = 3-6$.

Finally, Nagamine et al. (2010) showed that while their models with a constant $f_{\rm esc}^{\rm eff}$ fit the data well (in good agreement with our work), they obtain better fits using so-called 'duty cycle' models, in which $\frac{dn}{d\log L_\alpha} = \epsilon_{\rm DC} \frac{dn}{d\log\psi}\big|_{\psi = L_\alpha / k f_{\rm esc}^{\rm eff}}$. These models represent a scenario in which star forming galaxies only have non-zero $f_{\rm esc}^{\rm eff}$ for a fraction $\epsilon_{\rm DC}$ of their lifetimes. We note that this may also represent a scenario in which Lyα escapes anisotropically from galaxies, and in which $f_{\rm esc}^{\rm eff} > 0$ only along a fraction $\epsilon_{\rm DC}$ of the sightlines from them. The duty cycle parameter $\epsilon_{\rm DC}$ can also be incorporated in the $f_{\rm esc}^{\rm eff}$-PDF, simply by adding a Dirac-delta function at $f_{\rm esc}^{\rm eff} = 0$ (after which we must renormalize the full-PDF). We have repeated our analysis including a duty cycle of $\epsilon_{\rm DC} = 0.25$ into our $f_{\rm esc}^{\rm eff}$-PDF, and found that these models flatten the predicted luminosity functions, similarly to models with a non-zero scatter in $f_{\rm esc}^{\rm eff}$. These 'duty-cycle model' therefore provide somewhat better fits to the luminosity functions (for models with $\sigma = 0$), mostly because they improve the fits at the bright ends (just as our models with $\sigma = 0.5$), in agreement with Nagamine et al. (2010). Moreover, the best-fit *expectation values* of $f_{\rm esc}^{\rm eff}$ in these duty cycle models[12] are consistent with our those obtained previously.

4.3 Model Uncertainties

A potential caveat is that (some of) our adopted Lyα luminosity functions were constructed from narrow-band surveys. Such surveys do not only impose a Lyα flux cut, but in practice also a cut in Lyα equivalent width (EW). For example, Ouchi et al. (2008) adopt color-color criteria to select LAEs at $z = 3.1$ that translate (roughly) to EW $\gtrsim$64 Å. We may worry that this data-set therefore misses a significant fraction of Lyα emitting galaxies. In practise however, the equivalent width cut does not appear to affect determinations of the Lyα luminosity functions: Gronwall et al. (2007) present a luminosity function at $z = 3.1$ that agrees well with Ouchi et al. (2008), even though they effectively apply a different EW-cut of EW $\gtrsim$20 Å. Moreover, Cassata et al. (2010) derived their luminosity functions from a spectroscopic survey, which does not employ any EW cut. Our inferred value for $f_{\rm esc}^{\rm eff}$ from the Cassata et al. (2010) data was in fact lower than that for the Ouchi et al. (2008) data, which suggests that uncertainties associated with how different LAE samples are constructed are subdominant to other systematic uncertainties.

Our analysis uses Schechter functions to describe the star formation rate functions. Recenty, Salim & Lee (2012) have demonstrated that a superior fit to star formation functions can be obtained from 'Saunders' functions (introduced by Saunders et al. 1990), given by

$$\frac{dn}{d\psi} = \frac{\Phi_*}{\psi_*}\Big(\frac{\psi}{\psi_*}\Big)^{-\alpha} \exp\Big(\frac{-(\log[\psi/\psi_* + 1])^2}{2\sigma^2}\Big). \qquad (7)$$

For a fixed set of parameters (Φ_*, ψ_*, α), the Saunders function is identical to the Schechter function for $\psi \lesssim \psi_*$. However, at $\psi > \psi_*$ it cuts off as a Gaussian in log-space with a standard deviation σ, instead of the sharper exponential cut-off of the Schechter function in real-space. Salim & Lee (2012) show that Schechter functions typically predict (slightly) fewer galaxies at the largest ψ compared to the actual observations (see e.g. Fig 5 of Smit et al. 2012, and Fig 2 of Salim & Lee 2012), because of their exponential cut-off at $\psi > \psi_*$. For $\sigma = 0.5$ we can boost $dn/d\psi$ by a factor of $\sim$ a few at the high-ψ end, which may help resolve this issue. We repeated our analysis in which we replaced Schechter functions with Saunders functions (using $\sigma = 0.5$, and keeping the other parameters fixed), and found that this did not change our results at all. However, this may become more relevant in the future with larger LAE surveys which can probe down to larger Lyα luminosities (and likely larger values of ψ).

[11] To be precise, these models generate intrinsic Lyα luminosity functions, which give the number density of galaxies as a function of Lyα luminosity. This intrinsic Lyα luminosity function is practically the same as a star formation function.

[12] If we denote the expectation value of $f_{\rm esc}^{\rm eff}$ along sightlines (or during time-intervals) where $f_{\rm esc}^{\rm eff} > 0$ with $E(f_{\rm obs,DC})$. The overall expectation value is then given by $E(f_{\rm obs,DC}) = \epsilon_{\rm DC} E(f_{\rm esc}^{\rm eff})$.

4.4 Constraints on Models

In § 1 we mentioned that empirical constraints on $f_{\rm esc}^{\rm eff}$ may help us understand the basics of Lyα transport in and around galaxies. Our work has several implications:

• Our best-fit $f_{\rm esc}^{\rm eff} \sim 30-50\%$ at $z=6$. Models that have studied the impact of the IGM on the visibilty of Lyα photons emerging from galaxies at this redshift, consistently conclude that the alone IGM should transmit only $\mathcal{T}_{\rm IGM} \sim 5-30\%$ (e.g. Dijkstra et al. 2007; Iliev et al. 2008; Zheng et al. 2010; Dayal et al. 2011; Laursen et al. 2011) of photons through an ionized Universe at $z\sim 6$. Under the reasonable assumption that dust suppresses the emerging Lyα flux by an additional factor, these models would predict effective escape fractions that appear inconsistent with our inferred fraction (and also that of Hayes et al. 2011). A plausible reason for this discrepancy is that the models overestimate the IGM opacity, because they do not include the impact of outflows of optically thick (to Lyα photons) HI gas on the Lyα spectral line profile emerging from galaxies. Winds are known to redshift Lyα photons out of the line resonance, which can strongly increase the fraction of photons transmitted through the IGM (see e.g. Dijkstra & Wyithe 2010). It is interesting that current constraints on $f_{\rm esc}^{\rm eff}$ provide evidence for winds impacting the Lyα radiative transfer at $z\sim 6$.

• Our work has also shown that it is possible to reproduce Lyα luminosity functions with a constant (ψ-independent) $f_{\rm esc}^{\rm eff}$, in agreement with previous studies (e.g. Nagamine et al. 2010; Shimizu et al. 2011), although we have shown that this applies over a wider range of observed Lyα luminosities (by adding the data from Cassata et al. 2010 to the data from Ouchi et al. 2008 which was used in most previous analyses). We have shown that we 'flatten' the predicted luminosity functions by adding a dispersion in $f_{\rm esc}^{\rm eff}$ and/or a 'duty cycle' (as in Nagamine et al. 2010). This flattening can improve the fit to the observed luminosity function at the bright end. If we flatten the predicted luminosity functions even more (by increasing the dispersion, or reducing the duty cycle), then we need to invoke that $f_{\rm esc}^{\rm eff}$ decreases towards higher ψ, which appears to be favored by the observed increase 'Lyα fraction' towards fainter dropout galaxies (see § 3.2).

The two points combined favor a scenario in which Lyα photons escape anisotropically from LAEs through an outflowing ISM (as in e.g. Laursen & Sommer-Larsen 2007; Verhamme et al. 2012). This would provide a physical explanation for having a large scatter in $f_{\rm esc}^{\rm eff}$, and also for having the large values of $f_{\rm esc}^{\rm eff}$ that have been inferred from the data at $z\sim 6$.

5 CONCLUSIONS

In this paper, we have constrained the 'effective escape' fraction of Lyα photons, $f_{\rm esc}^{\rm eff}$, which is defined as the ratio of the observed Lyα luminosity of a galaxy to its intrinsic Lyα luminosity. This ratio is often referred to in the literature simply as an escape fraction. In § 4.1 we have argued why we caution against universal usage of the term escape fraction, and why it helps to distinguish between an escape fraction and an effective escape fraction.

We have constrained the effective escape fraction by converting observed star formation functions to observed Lyα luminosity functions. This conversion depends directly on $f_{\rm esc}^{\rm eff}$, and we use observed Lyα luminosity functions at $z=0.35$, $z=3.1$, $z=3.7$, and $z=5.7$ to get constraints on $f_{\rm esc}^{\rm eff}$ at these redshifts. We have explored models in which $f_{\rm esc}^{\rm eff}$ takes on a single value (§ 3.1), and in which $f_{\rm esc}^{\rm eff}$ has a dispersion (§ 3.2). Models which include a dispersion predict flatter luminosity functions, which appear to be in better agreement with the observations. We note that the flattening predicted by these models cannot be captured by Schechter functions (a Saunders function as in Eq 7 would likely be more appropriate).

We found that the effective escape fraction (or its expectation value in a distribution) $f_{\rm esc}^{\rm eff} \sim 1-3\%$ at $z=0$, and that it increases to $f_{\rm esc}^{\rm eff} \sim 10\%$ at $z=3-4$, and to $z=35-50\%$ at $z=6$ (see Fig 2). Eq 6 provides a convenient fitting formula that encapsulates our main findings. Our results are consistent with previous work (e.g. Hayes et al. 2010; Blanc et al. 2011; Hayes et al. 2011), except at $z\sim 0.35$ where our inferred $f_{\rm esc}^{\rm eff}$ is higher than previous works. We have argued in § 3 that this difference may be a result of the systematic uncertainty on $f_{\rm esc}^{\rm eff}$ becoming increasingly large for very small $f_{\rm esc}^{\rm eff}$ in previous analyses. We argued in § 4.4 that our constraint on $f_{\rm esc}^{\rm eff}$ at $z\sim 6$ appears higher than predicted by models that do not include winds. This hints at the importance of winds in the Lyα transfer process even at this high redshift.

We have shown that we can reproduce observed Lyα luminosity functions in individual redshift bins with a constant - i.e. independent of ψ- $f_{\rm esc}^{\rm eff}$ over up to two orders in ψ and Lyα luminosity (see Fig 2), in agreement with previous work. We require $f_{\rm esc}^{\rm eff}$ to decrease with ψ - as appears to be favored by observations of drop-out galaxies (see § 3.2)- only in models which include a large scatter ($\sigma \gtrsim 1.0$ dex) in $f_{\rm esc}^{\rm eff}$, or in which star forming galaxies only have a non-zero $f_{\rm esc}^{\rm eff}$ for a fraction $\epsilon_{\rm DC}$ of their life-time and/or a fraction of sightlines (see § 4.3).

We anticipate that observations of Lyα emitting galaxies in the near future (e.g. with MUSE[13], Hyper Suprime-Cam[14] and by HETDEX) will determine the Lyα luminosity functions over a wider range of luminosities, and reduce their systematic uncertainties. This may allow for better constraints on $f_{\rm esc}^{\rm eff}$, and its PDF. As illustrated in the discussion in § 4.4, constraints on the $f_{\rm esc}^{\rm eff}$-PDF yield valuable basic insights into Lyα transfer process on small scales. Perhaps this is more speculative, but the possible dependence of these luminosity functions on the surface brightness threshold of the survey would shed light on the presence of spatially extended Lyα halos around star forming galaxies, which encode valuable information on cold gas around galaxies (e.g Zheng et al. 2011; Dijkstra & Kramer 2012; Jeeson-Daniel et al. 2012).

Acknowledgements We thank an anonymous referee for a prompt report that improved the content of this paper significantly, and for insisting we should not use the name we initially had for the quantity now called 'effective escape fraction'.

[13] http://www.eso.org/sci/facilities/develop/instruments/muse.html
[14] http://www.naoj.org/Projects/HSC/

REFERENCES

Andrae, R. 2010, arXiv:1009.2755
Barger, A. J., Cowie, L. L., & Wold, I. G. B. 2012, ApJ, 749, 106
Barnes, L. A., Haehnelt, M. G., Tescari, E., & Viel, M. 2011, MNRAS, 416, 1723
Bell, E. F., Zheng, X. Z., Papovich, C., et al. 2007, ApJ, 663, 834
Blanc, G. A., Adams, J. J., Gebhardt, K., et al. 2011, ApJ, 736, 31
Bothwell, M. S., Kenicutt, R. C., Johnson, B. D., et al. 2011, MNRAS, 415, 1815
Cantalupo, S., Lilly, S. J., & Haehnelt, M. G. 2012, MNRAS, 425, 1992
Cassata, P., Le Fèvre, O., Garilli, B., et al. 2011, A&A, 525, A143
Cowie, L. L., Barger, A. J., & Hu, E. M. 2010, ApJ, 711, 928
Dayal, P., Maselli, A., & Ferrara, A. 2011, MNRAS, 410, 830
Deharveng, J.-M., Small, T., Barlow, T. A., et al. 2008, ApJ, 680, 1072
Dijkstra, M., Haiman, Z., & Spaans, M. 2006, ApJ, 649, 14
Dijkstra, M., Lidz, A., & Wyithe, J. S. B. 2007, MNRAS, 377, 1175
Dijkstra, M., & Westra, E. 2010, MNRAS, 401, 2343
Dijkstra, M., & Wyithe, J. S. B. 2010, MNRAS, 408, 352
Dijkstra, M., & Kramer, R. 2012, MNRAS, 424, 1672
Dijkstra, M., & Wyithe, J. S. B. 2012, MNRAS, 419, 3181
Feldmeier, J., Hagen, A., Ciardullo, R., et al. 2013, arXiv:1301.0462
Forero-Romero, J. E., Yepes, G., Gottlöber, S., et al. 2011, MNRAS, 415, 3666
Fynbo, J. U., Möller, P., & Thomsen, B. 2001, A&A, 374, 443
Gronwall, C., et al. 2007, ApJ, 667, 79
Haiman, Z., & Spaans, M. 1999, ApJ, 518, 138
Hansen, M., & Oh, S. P. 2006, MNRAS, 367, 979
Hayes, M., Östlin, G., Schaerer, D., et al. 2010, *Nature*, 464, 562
Hayes, M., Schaerer, D., Östlin, G., et al. 2011, ApJ, 730, 8
Hayes, M., Östlin, G., Schaerer, D., et al. 2013, ApJL, 765, L27
Hill, G. J., Gebhardt, K., Komatsu, E., et al. 2008, Panoramic Views of Galaxy Formation and Evolution, 399, 115
Iliev, I. T., Shapiro, P. R., McDonald, P., Mellema, G., & Pen, U.-L. 2008, MNRAS, 391, 63
Iye, M., Ota, K., Kashikawa, N., et al. 2006, *Nature*, 443, 186
Jeeson-Daniel, A., Ciardi, B., Maio, U., et al. 2012, MNRAS, 424, 2193
Jiang, L., Egami, E., Fan, X., et al. 2013, arXiv:1303.0027
Johnson, J. L., Greif, T. H., Bromm, V., Klessen, R. S., & Ippolito, J. 2009, MNRAS, 399, 37
Kennicutt, R. C., Jr. 1998, ARA&A, 36, 189
Kobayashi, M. A. R., Totani, T., & Nagashima, M. 2007, ApJ, 670, 919
Laursen, P., & Sommer-Larsen, J. 2007, ApJL, 657, L69
Laursen, P., Sommer-Larsen, J., & Razoumov, A. O. 2011, ApJ, 728, 52
Laursen, P., Duval, F., & Ostlin, G. 2012, arXiv:1211.2833
Le Delliou, M., Lacey, C. G., Baugh, C. M., & Morris, S. L. 2006, MNRAS, 365, 712
Malhotra, S., & Rhoads, J. E. 2004, ApJL, 617, L5
Matsuda, Y., Yamada, T., Hayashino, T., et al. 2012, MNRAS, 425, 878
Nagamine, K., Ouchi, M., Springel, V., & Hernquist, L. 2010, PASJ, 62, 1455
Neufeld, D. A. 1990, ApJ, 350, 216
Ostlin, G., Hayes, M., Kunth, D., et al. 2009, AJ, 138, 923
Ota, K., Iye, M., Kashikawa, N., et al. 2010, ApJ, 722, 803
Ouchi, M., Shimasaku, K., Akiyama, M., et al. 2008, ApJS, 176, 301
Partridge, R. B., & Peebles, P. J. E. 1967, ApJ, 147, 868
Raiter, A., Schaerer, D., & Fosbury, R. A. E. 2010, A&A, 523, A64
Rauch, M., Haehnelt, M., Bunker, A., et al. 2008, ApJ, 681, 856
Rhoads, J. E., Hibon, P., Malhotra, S., Cooper, M., & Weiner, B. 2012, ApJL, 752, L28
Salim, S., & Lee, J. C. 2012, ApJ, 758, 134
Saunders, W., Rowan-Robinson, M., Lawrence, A., et al. 1990, MNRAS, 242, 318
Schaerer, D. 2003, A&A, 397, 527
Shimizu, I., Yoshida, N., & Okamoto, T. 2011, MNRAS, 418, 2273
Smit, R., Bouwens, R. J., Franx, M., et al. 2012, ApJ, 756, 14
Stark, D. P., Ellis, R. S., Chiu, K., Ouchi, M., & Bunker, A. 2010, MNRAS, 408, 1628
Steidel, C. C., Bogosavljević, M., Shapley, A. E., et al. 2011, ApJ, 736, 160
Tasitsiomi, A. 2006, ApJ, 645, 792
Verhamme, A., Schaerer, D., Atek, H., & Tapken, C. 2008, A&A, 491, 89
Verhamme, A., Dubois, Y., Blaizot, J., et al. 2012, A&A, 546, A111
Yajima, H., Li, Y., Zhu, Q., et al. 2012, ApJ, 754, 118
Yajima, H., Li, Y., Zhu, Q., et al. 2012, arXiv:1209.5842
Zheng, Z., & Miralda-Escudé, J. 2002, ApJ, 578, 33
Zheng, Z., Cen, R., Trac, H., & Miralda-Escudé, J. 2010, ApJ, 716, 574
Zheng, Z., Cen, R., Weinberg, D., Trac, H., & Miralda-Escudé, J. 2011, ApJ, 739, 62